

Toward real maximally path-entangled N -photon-state sources

Milena D'Angelo,¹ Augusto Garuccio,^{1,2} and Vincenzo Tamma^{1,3}

¹*Dipartimento Interateneo di Fisica, Università degli Studi di Bari, 70100 Bari, Italy*

²*Istituto Nazionale Di Fisica Nucleare, sez. di Bari, 70100 Bari, Italy*

³*Department of Physics, University of Maryland, Baltimore County, Baltimore, Maryland 21250, USA*

(Received 1 February 2008; revised manuscript received 12 March 2008; published 17 June 2008)

Path-entangled N -photon systems described by NOON states are the main ingredient of many quantum information and quantum imaging protocols. Our analysis aims to lead the way toward the implementation of both NOON-state sources and their applications. To this end, we study the functionality of “real” NOON-state sources by quantifying the effect real experimental apparatuses have on the actual generation of the desired NOON state. In particular, since the conditional generation of NOON states strongly relies on photon counters, we evaluate the dependence of both the reliability and the signal-to-noise ratio of “real” NOON-state sources on detection losses. We find a surprising result: NOON-state sources relying on nondetection are much more reliable than NOON-state sources relying on single-photon detection. Also the comparison of the resources required to implement these two protocols comes out to be in favor of NOON-state sources based on nondetection. A scheme to improve the performances of “real” NOON-state sources based on single-photon detection is also proposed and analyzed.

DOI: [10.1103/PhysRevA.77.063826](https://doi.org/10.1103/PhysRevA.77.063826)

PACS number(s): 42.50.Dv, 03.65.Ud, 03.67.Bg

I. INTRODUCTION

In recent years, much attention has been given to the production of a particular kind of path-entangled N -photon systems, the so-called NOON states [1–15]

$$|\text{NOON}^\theta\rangle_{a,b} = \frac{1}{\sqrt{2}}(|N,0\rangle_{a,b} + e^{i\theta}|0,N\rangle_{a,b}), \quad (1)$$

where $|N,0\rangle_{a,b}$ indicates an N -photon Fock state in mode a and vacuum in mode b , with a and b being two nonoverlapping spatial modes. The interest in the production of NOON states arises from the crucial role they play in many quantum information protocols [16], as well as in quantum optical lithography [17] and quantum metrology [1,6,9–11,18].

A *NOON-state source* is a production scheme able to generate NOON states and to make them available for further use. The most feasible optical NOON-state sources proposed so far are based on linear optics and projective measurements: quantum interference effects occurring in a generalized Hong-Ou-Mandel–Shih-Alley (HOM-SA) interferometer [19] are combined with nondestructive projective measurements (NDPMs) to transform an input Fock state into the desired NOON state [3–6]. In particular, both Zou, *et al.* [4] and Fiurásek [5] have proposed a NOON-state source requiring N single-photon input states and relying on N simultaneous detections of vacuum (or nondetections). On the other hand, Kok, Lee, and Dowling [6], considering the technical difficulties connected to the detection of vacuum, proposed to double the number of input photons and to replace the N vacuum detections by N single-photon detections. The nondetection protocol was seen as being too sensitive to detection losses as well as to all other possible reasons why a detector may not click (e.g., either the laser or the detectors are off). Both these schemes will be described in more detail in Sec. II.

The reliability and signal-to-noise ratio as well as the feasibility of NOON-state sources are basic requirements for all

applications relying on NOON states. In the attempt to lead the way toward the implementation of both NOON-state sources and their applications, we aim to study the actual functionality of the NOON-state sources, described above, under real experimental conditions. In particular, we quantitatively evaluate both the reliability and the signal-to-noise ratio of “real” NOON-state sources by taking into account the effect real experimental apparatuses have on the actual generation of the desired NOON states. It is nowadays well known how deeply the theoretical predictions of quantum mechanics may change when going from ideal to actual experimental situations; the difficulties related to the implementation of a loophole-free test of Bell’s inequality are a quite striking demonstration of the crucial role played by the nonunitary detection efficiency in generating such a deep change [20]. Following this idea and considering that the NOON-state sources we are considering strongly rely on projective measurements, we evaluate the reliability (Sec. III) of “real” NOON-state sources in terms of the nonunitary detection efficiency of photon counters. Note that we refer to “real” NOON-state sources because we account for the effect of real detection apparatuses; however, a real NOON-state source will also involve real photon sources and real optical elements, which in this work we consider to be ideal. This analysis, carried out for both the nondetection (Sec. III A) and the single-photon detection (Sec. III B) schemes, leads us to a quite surprising result (Sec. III C): “real” NOON-state sources relying on nondetection are much less sensitive to detection losses than “real” NOON-state sources relying on single-photon detection. To better understand the reason behind this result, we propose and analyze a modified scheme for improving the performances of the NOON-state source based on single-photon detection (Sec. III D). We then discuss the feasibility of all these NOON-state sources by comparing the resources they require with the available technology (Sec. IV). Furthermore, we discuss the nature of the optical system effectively produced by “real” NOON-state sources (Sec. V) and evaluate their characteristic signal-to-

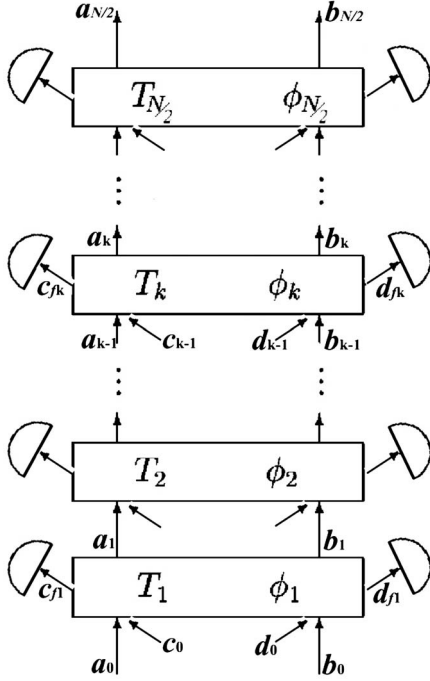


FIG. 1. NOON-state source: generic scheme for producing NOON states (with an even number N of photons) by exploiting nondestructive projective measurements. Each cell includes a phase shifter (ϕ_k), two identical beam splitters with transmission probability T_k , and two photodetectors.

noise ratio (Sec. VI). We then summarize our results and draw some conclusions (Sec. VII).

II. IDEAL NOON-STATE SOURCES

Let us start by describing the protocol of NOON-state sources. We will only consider schemes producing NOON states with an even number N of photons, which are indeed characterized by a production probability higher than in the odd case [5]. Both the nondetection and single-photon detection protocols involve a sequence of $\frac{N}{2}$ cells, as shown in Fig. 1. Each k cell (with $k=1, \dots, N/2$) is characterized by four input modes (a_{k-1} , b_{k-1} , c_{k-1} , and d_{k-1}) and four output modes (a_k , b_k , c_{fk} , and d_{fk}), two of which (a_k and b_k) enter into the $k+1$ cell, while the other two (c_{fk} and d_{fk}) impinge on photon counters. Each cell is characterized by both a phase shifter ($\phi_k = \frac{2\pi k}{N}$) and a pair of identical beam splitters with transmission probability T_k . We shall indicate the input and output states of the whole apparatus as $|\psi_{\text{in}}\rangle \doteq |\psi_{\text{in}}\rangle_{a_0, b_0, c_0, d_0, \dots, c_{N/2-1}, d_{N/2-1}}$ and $|\psi_{\text{out}}\rangle \doteq |\psi_{\text{out}}\rangle_{a_{N/2}, b_{N/2}, c_{f1}, d_{f1}, \dots, c_{fN/2}, d_{fN/2}}$, respectively. All single-photon detectors, together, perform the NDPM responsible for the collapse of the overall output state $|\psi_{\text{out}}\rangle$ into the desired NOON state $|\text{NOON}^\theta\rangle_{a_{N/2}, b_{N/2}}$, with $\theta=0$ when $\frac{N}{2}$ is odd and $\theta=\pi$ when $\frac{N}{2}$ is even.

The projective measurement consists of N simultaneous nondetections (Nnd), in the nondetection scheme, and of N simultaneous single-photon detections (Nsd), in the single-photon detection scheme. The projectors describing such ideal measurements are, respectively,

$$\hat{\Pi}_{\text{Nnd}} \doteq \bigotimes_{k=1}^{N/2} (|0\rangle_{c_{fk}c_{fk}} \langle 0| \otimes |0\rangle_{d_{fk}d_{fk}} \langle 0|) \quad (2)$$

and

$$\hat{\Pi}_{\text{Nsd}} \doteq \bigotimes_{k=1}^{N/2} (|1\rangle_{c_{fk}c_{fk}} \langle 1| \otimes |1\rangle_{d_{fk}d_{fk}} \langle 1|), \quad (3)$$

where the symbol $\bigotimes_{k=1}^{N/2}$ indicates the tensor product of the projectors associated with each k cell.

III. “REAL” NOON-STATE SOURCES AND THEIR RELIABILITY

In reality, due to detection losses naturally occurring in real photodetectors, the number of detected photons may differ from the number of photons impinging on the photodetector; hence, real measurements do not allow precise knowledge about the impinging photon state.

For instance, when neglecting dark counts, nondetection occurs with certainty when no photons impinge on a detector, whether it is ideal or real; however, a real detector, characterized by single-photon detection efficiency $\eta < 1$, has a probability $(1-\eta)^n$ of not detecting $n \geq 1$ photons impinging on it. Hence, in order to describe a real detector aiming to detect vacuum, we need to replace the projector of Eq. (2) with the measurement operator [21]

$$\hat{\Pi}_{\text{Nnd real}}(\eta) \doteq \bigotimes_{k=1}^{N/2} \left[\sum_{n=0}^{\infty} (1-\eta)^n |n\rangle_{c_{fk}c_{fk}} \langle n| \otimes \sum_{n=0}^{\infty} (1-\eta)^n |n\rangle_{d_{fk}d_{fk}} \langle n| \right]. \quad (4)$$

When dealing with a real photodetector having single-photon detection efficiency η and unable to discriminate the number of detected photons [e.g., a standard single-photon counting module (SPCM) based on an avalanche photodiode [22]], the measurement operator of Eq. (4) is one of the two elements composing the positive-operator-valued measurement (POVM) describing such a detector. At the same time, the measurement operator of Eq. (4) is one of the $N+1$ elements composing the POVM describing a photon-number resolving detector (e.g., an energy detector [23]), characterized by a single-photon detection efficiency η and able to resolve $N = 1, 2, \dots$ photons. In other words, nondetection can be performed by both SPCM and energy detectors.

On the other hand, a real photon counter has a probability η of detecting a single photon impinging on it and a probability $n\eta(1-\eta)^{(n-1)}$ of detecting a single photon even though $n \geq 2$ photons impinged on it. Hence, a real photon counter aiming to detect single photons cannot be described by the projector of Eq. (3), but rather by the measurement operator

$$\hat{\Pi}_{\text{Nsd real}}(\eta) \doteq \otimes_{k=1}^{N/2} \left[\sum_{n=1}^{\infty} n \eta (1-\eta)^{n-1} |n\rangle_{c_{fk}d_{fk}} \langle n| \right] \otimes \left[\sum_{n=1}^{\infty} n \eta (1-\eta)^{n-1} |n\rangle_{d_{fk}c_{fk}} \langle n| \right]. \quad (5)$$

Note that, in this case, the measurement operator of Eq. (5) can only be seen as one of the $N+1$ elements composing the POVM describing a photon-number resolving detector, characterized by a single-photon detection efficiency η and able to register the number $N=1, 2, \dots$ of detected photons.

Both measurement operators of Eqs. (4) and (5) have been written under the assumption that the detection efficiency $\eta < 1$ is the same for all photodetectors in the setup. Note that both measurement operators involve weighted sums of all the projectors corresponding to the detection of n photons in mode c_{fk} and m photons in mode d_{fk} , even though the weighting probabilities are clearly different in the two schemes. Hence, the effect of detection losses is to force the overall output state $|\psi_{\text{out}}\rangle$ to collapse into any possible state $|\psi_{\text{out}}\rangle_{a_{N/2}, b_{N/2}}$ associated with the *real* (i.e., imperfect, unsharp) measurement; in general, the produced state $|\psi_{\text{out}}\rangle_{a_{N/2}, b_{N/2}}$ differs from the desired NOON state, as we shall see in more details in Sec. V. We shall thus define the reliability of a NOON-state source as the conditional probability of producing a NOON state upon *real* measurement, which is

$$R_{\text{MO real}}(\eta) \doteq \frac{P_{(\text{NOON} \cap \text{MO real})}(\eta)}{P_{(\text{MO real})}(\eta)}, \quad (6)$$

where

$$P_{(\text{MO real})}(\eta) = \langle \psi_{\text{out}} | [\hat{\Pi}_{\text{MO real}}(\eta) \otimes \hat{1}] | \psi_{\text{out}} \rangle \quad (7)$$

is the probability associated with the real measurement, as described by the measurement operator (MO) of either Eq. (4) or (5); $\hat{1}$ is the identity operator acting on channels $a_{N/2}$ and $b_{N/2}$. In Eq. (6), $P_{(\text{NOON} \cap \text{MO real})}(\eta)$ is the probability associated with both the real measurement of interest (whether MO real=Nnd real or Nsd real) and NOON-state production, which is

$$P_{(\text{NOON} \cap \text{MO real})} = \langle \psi_{\text{out}} | [\hat{\Pi}_{\text{MO real}}(\eta) \otimes |\text{NOON}\rangle\langle\text{NOON}|] \times | \psi_{\text{out}} \rangle. \quad (8)$$

In order to evaluate the actual functionality of “real” NOON-state sources, in Secs. III A and III B, we will quantify the effect detection losses have on the reliability of the two NOON-state sources described so far. To this end, the overall output state $|\psi_{\text{out}}\rangle$ appearing in both Eqs. (7) and (8) will be evaluated by propagating the ideal input state through the linear optical setup, assuming all optical elements to be perfect.

Before entering into the details of this calculation, it is worth emphasizing that the measurement operators introduced in Eqs. (4) and (5) describe measurements performed by real detectors, as far as their nonunitary detection efficiency is concerned, but do not account for their dark counts (i.e., a click occurs even though no photons impinge on the

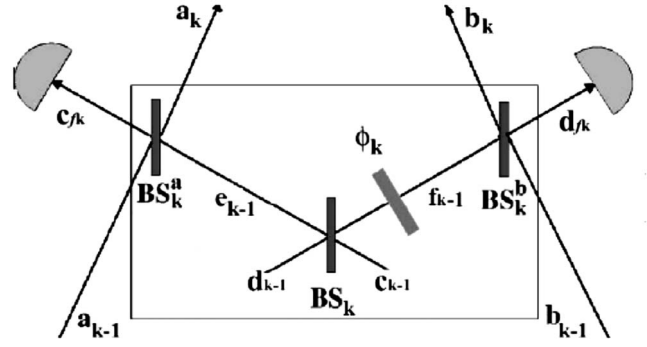


FIG. 2. Generic k (with $k=1, 2, \dots, \frac{N}{2}$) cell of the NOON-state source relying on nondetection, as proposed by Fiurásek [5]. The input state of the generic 50:50 beam splitter BS_k is $|1, 1\rangle_{c_{k-1}, d_{k-1}}$, while modes a_{k-1} and b_{k-1} are empty.

detector). This is not an issue when dealing with the nondetection protocol. In fact, this scheme leads to the potential production of a NOON state only upon no-click events; this makes both the measurement operator of interest and the reliability of this scheme completely unaffected by dark counts. However, in the single-photon detection protocol, dark counts are as misleading as fake single-photon detections (i.e., two or more photons impinge on the detectors, but only one is detected); hence, to evaluate the actual reliability of the single-photon detection protocol, one should add to the measurement operator of Eq. (5) a projector over vacuum [similar to the one given in Eq. (2)], with the appropriate weighting probability. Here we will not enter into the details of this calculation, but it is important to keep in mind that the actual reliability of the NOON-state source based on single-photon detection is certainly lower than the one we are going to evaluate, due to dark counts.

A. Reliability of a “real” NOON-state source based on nondetection

Let us start by considering the nondetection protocol, whose generic k cell is depicted in Fig. 2 [5]. Modes a_0 and b_0 are empty, while $N/2$ pairs of single-photon Fock states $|1, 1\rangle_{c_{k-1}, d_{k-1}}$ impinge on each balanced beam splitter BS_k , with $k=1, \dots, N/2$. In order to maximize the probability of N simultaneous nondetections (whether ideal or real) in all channels c_{fk} and d_{fk} , the transmission probability of the identical beam splitters BS_k^a and BS_k^b is chosen to be [5]

$$T_k = \frac{k-1}{k}. \quad (9)$$

After propagating the overall input state ($|\psi_{\text{in}}\rangle = |0, 0, 1, 1, \dots, 1, 1, \dots, 1, 1\rangle_{a_0, b_0, c_0, d_0, \dots, c_{k-1}, d_{k-1}, \dots, c_{N/2-1}, d_{N/2-1}}$) through the optical setup of Figs. 1 and 2, we will evaluate the reliability $R_{\text{Nnd real}}(\eta)$ of the NOON-state source relying on nondetection by plugging both the resulting output state $|\psi_{\text{out}}\rangle$ and the measurement operator of Eq. (4) into Eqs. (7) and (8), with MO real=Nnd real, and then (6). We will do so by considering three special cases: $N=2, 4$, and 6.

In the two-photon case ($N=2$), the NOON-state source under consideration reduces to a single cell containing a

standard HOM-SA interferometer. In fact, since Eq. (9) gives a null transmission probability ($T_1=0$) for both beam splitters BS_1^a and BS_1^b , the pair of single-photon detectors in this single-cell apparatus does not play any role in producing the desired two-photon NOON state. The reliability of this NOON-state source is thus independent of the detection efficiency and is simply unitary ($R_{2nd\ real}=1$), as it would be in the ideal case of perfect detectors. In the four- and six-

photon cases, the scheme is composed by two and three cells, respectively, and the corresponding reliabilities are found to be

$$R_{4nd\ real}(\eta) = \frac{3}{(2-\eta)^2(4-4\eta+3\eta^2)} \quad (10)$$

and

$$R_{6nd\ real}(\eta) = \frac{10}{324 - 1296\eta + 2376\eta^2 - 2448\eta^3 + 1467\eta^4 - 480\eta^5 + 67\eta^6}. \quad (11)$$

The three results obtained so far are reported in Fig. 4, below, where the reliability of the “real” NOON-state source based on nondetection is plotted as a dash-dotted line versus the detection efficiency η .

B. Reliability of a “real” NOON-state source based on single-photon detection

Let us now consider the single-photon detection protocol for generating N -photon NOON states, whose generic k cell (with $k=1, 2, \dots, \frac{N}{2}$) is depicted in Fig. 3 [6]. The input state is now $|\psi_{in}\rangle = |N, N\rangle_{a_0, b_0}$, indicating that all c_{k-1} and d_{k-1} modes are empty; in each cell, the input modes a_{k-1} and b_{k-1} are thus mixed with vacuum on the corresponding beam splitters BS_k^a and BS_k^b , respectively. In order to maximize the probability of N simultaneous single-photon detections in channels c_{fk} and d_{fk} , the transmission probability of the two identical beam splitters BS_k^a and BS_k^b is now chosen to be [6]

$$T_k = \frac{N-k}{N-k+1}. \quad (12)$$

By propagating the input state $|\psi_{in}\rangle$ through the entire linear optical setup of Figs. 1 and 3, one can find the output state

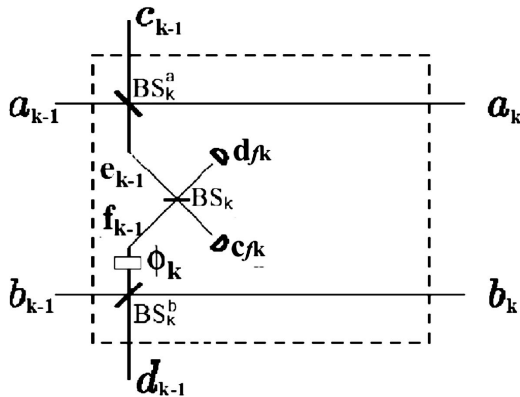


FIG. 3. Generic k (with $k=1, 2, \dots, \frac{N}{2}$) cell of the NOON-state source relying on single-photon detection, as proposed by Kok *et al.* [6]. The overall input state is $|\psi_{in}\rangle = |N, N\rangle_{a_0, b_0}$, indicating that modes c_{k-1} and d_{k-1} are empty.

$|\psi_{out}\rangle$ and employ it, together with the measurement operator of Eq. (5), to evaluate both the probabilities of Eqs. (7) and (8), with $MO_{real} = Nsd_{real}$; the results can then be plugged into Eq. (6) to obtain the reliability of the “real” single-photon detection protocol. For the three cases $N=2, 4$, and 6 , we find the reliability of this NOON-state source to be

$$R_{Nsd\ real}(\eta) = (2-\eta)^{-N}. \quad (13)$$

The result of Eq. (13) is shown in Fig. 4, where the dashed line indicates the reliability of the “real” NOON-state source based on single-photon detection as a function of the efficiency η of the photon counters involved in the scheme.

C. Comparison of the results

We have evaluated the effect detection losses have on the reliability of optical NOON-state sources for $N=2, 4, 6$. Figure 4 indicates that the reliability of NOON-state sources is strongly affected by detection losses and increases for increasing values of the efficiency, as expected. In this respect, it is worth reminding ourselves that the unitary reliability characterizing the nondetection scheme in the case $N=2$ is simply due to the fact that the first cell of this scheme does not employ the detectors in channels c_{fk} and d_{fk} , as we will further discuss in the following section. Furthermore, inspection of Fig. 4 indicates that, for any realistic value of the efficiency ($0 < \eta < 1$), the reliability of NOON-state sources decreases as the number of photons, N , increases; this is obviously due to the increasing number of detectors involved in the scheme.

It is interesting to note that, different from previous expectations, the reliability of NOON-state sources based on nondetection ($R_{Nnd\ real}$) is always larger than the reliability of NOON-state sources based on single-photon-detection ($R_{Nsd\ real}$). In particular, the difference between the two reliabilities remains significant within the range of typical values of the detection efficiency (i.e., $0.6 < \eta < 0.9$).

D. Modified NOON-state source based on single-photon detection and its reliability

Considering the different number of detectors effectively involved in the two schemes considered so far, one may ex-

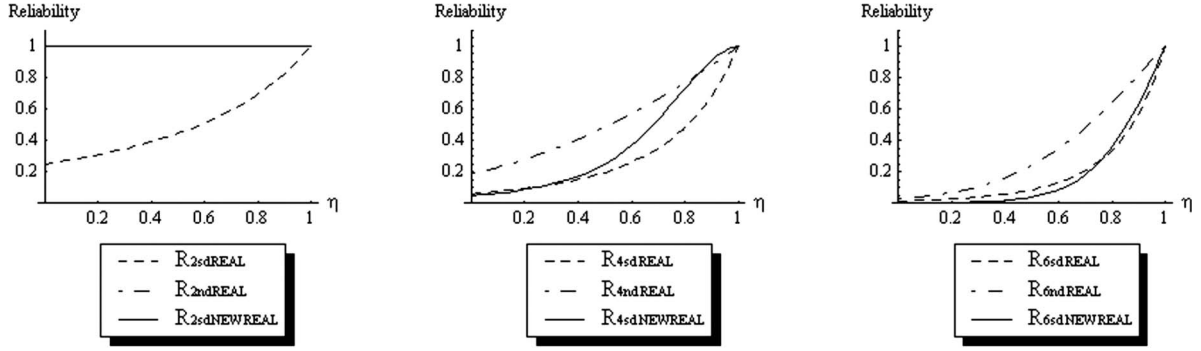


FIG. 4. Comparison of the reliability characterizing “real” N -photon NOON-state sources based on N single-photon detections ($R_{Nsd \text{ real}}$, dashed line) and N nondetections ($R_{Nnd \text{ real}}$, dash-dotted line) for the three cases $N=2, 4, 6$ from left to right. The solid line is the reliability of the modified single-photon detection scheme ($R_{Nsd \text{ new real}}$): the first cell of the original scheme is made identical to the first cell of the nondetection scheme in such a way so as to reduce the total number of detectors from N to $N-2$.

pect the reliability of the single-photon detection scheme to improve when transforming its first cell into a standard HOM-SA interferometer, similar to the first cell of the nondetection scheme; in this way, the number of detectors would be reduced from N to $N-2$. Based on this idea, we are going to modify the original single-photon detection protocol and evaluate its reliability as a function of the detection efficiency.

In the modified single-photon detection protocol all cells, besides the first one, are identical to the cells in the original scheme (Fig. 3 for $k=2, 3, \dots, N/2$); the first cell, on the other hand, is identical to the first cell of the nondetection protocol (Fig. 2 for $k=1$). For such a scheme to be a NOON-state source, the input state $|\psi_{\text{in}}\rangle$ needs to be modified with respect to the original single-photon detection scheme: in analogy with the nondetection scheme, two independent single photons enter the first cell through modes c_0 and d_0 (i.e., $|\psi_{\text{in}}\rangle_{1st \text{ cell}} = |0, 0\rangle_{a_0, b_0} |1, 1\rangle_{c_0, d_0}$), giving rise to a NOON state with $N=2$ in the output modes a_1 and b_1 ; while entering the second cell, the NOON state generated by the first cell is mixed with a pair of two independent photons entering

through modes c_1 and d_1 [i.e., $|\psi_{\text{in}}\rangle_{2nd \text{ cell}} = 1/\sqrt{2}(|20\rangle_{a_1, b_1} - |02\rangle_{a_1, b_1})|2, 2\rangle_{c_1, d_1}$]; all the remaining cells keep mixing the output state of the previous cell (modes a_{k-1}, b_{k-1}) with a pair of two independent photons entering through modes c_{k-1} and d_{k-1} , with $k=2, 3, \dots, N/2$. The overall input state is thus given by: $|\psi_{\text{in}}\rangle = |1, 1\rangle_{c_0, d_0} \otimes_{k=2}^{N/2} |2, 2\rangle_{c_{k-1}, d_{k-1}}$; by propagating this input state through the optical setup described above, it is easy to show that, in the ideal case of perfect detectors, a NOON state is generated by this scheme upon $N-2$ simultaneous single-photon detections, two in each k cell, with $k=2, 3, \dots, N/2$. By taking into account the detection efficiency [i.e., by employing the measurement operator of Eq. (5)], we have evaluated the effective reliability of this modified single-photon detection scheme for producing NOON states, with $N=2, 4, 6$ photons; the results

$$R_{2sd \text{ new real}}(\eta) = 1, \quad (14)$$

$$R_{4sd \text{ new real}}(\eta) = \frac{4}{81 - 216\eta + 207\eta^2 - 72\eta^3 + 4\eta^4}, \quad (15)$$

$$R_{6sd \text{ new real}}(\eta) \approx \frac{0.00505}{2.51 - 12.3\eta + 25.8\eta^2 - 29.2\eta^3 + 19.0\eta^4 - 6.68\eta^5 + \eta^6} \quad (16)$$

are plotted as the solid line in Fig. 4.

The new scheme is obviously characterized by perfect reliability in the case of $N=2$. An interesting result occurs in the case $N=4$: the modified single-photon detection scheme is not only more reliable than the original single-photon detection scheme (dashed line in Fig. 4), but is even more reliable than the nondetection protocol (dash-dotted line in Fig. 4) for values of the efficiency higher than 0.8. However, Fig. 4 clearly indicates that the improved reliability of the new scheme is significant only for small photon numbers: already in the case $N=6$, its reliability ($R_{6sd \text{ new real}}$) is very

close to the reliability of the original single-photon detection scheme ($R_{6sd \text{ real}}$) and remains very small with respect to the one characterizing the nondetection scheme ($R_{6nd \text{ real}}$). In other words, the different number of detectors involved in the nondetection and single-photon detection protocols ($N-2$ and N , respectively) is responsible for the lower reliability of the latter only when dealing with NOON states with $N=2$ and $N=4$ photons; for larger photon numbers, the single-photon detection scheme remains less reliable than the nondetection scheme, whether it employs N or $N-2$ detectors.

IV. FEASIBILITY OF NOON-STATE SOURCES

The larger reliability of “real” NOON-state sources based on nondetection is not the only reason for favoring this protocol with respect to the one based on single-photon detection. In fact, in view of the practical implementation of NOON-state sources, one should also take into account that the resources required by the nondetection protocol are much more affordable than in the single-photon detection protocol.

First, as mentioned in Sec. III, the nondetection scheme works well even with single-photon counting modules [22], sensitive to single photons, but unable to resolve the number of detected photons, while the single-photon detection scheme strongly relies on the much less practical photon-number resolving detectors [23].

Second, as emphasized earlier, the nondetection protocol has the advantage of being unaffected by the dark counts of the detectors.

Third, the nondetection protocol requires N single-photon Fock states, while the single-photon detection protocol requires one pair of N -photon Fock states, in its original version, and a pair of single-photons plus $N-2$ two-photon Fock states, in the modified version. In this respect, the difficulty connected with the realization of the single-photon detection protocol is not the mere request of twice as many photons as in the nondetection scheme; the biggest concern is rather the actual availability of the required photon sources. In fact, even though on demand single-photon sources are not yet available, their realization is expected to be more immediate than the realization of on-demand N -photon sources, with $N \geq 2$. In addition, while single-photon Fock states could be potentially mimicked by either weak-laser pulses or conditioned spontaneous parametric down-conversion, there is no easy way to simulate a pair of N -photon Fock states, with

$N \geq 2$. In this respect, it would certainly be interesting to evaluate the effect imperfect input states have on the reliability of NOON-state sources; this discussion will be at the center of future works.

V. OPTICAL SYSTEM EFFECTIVELY PRODUCED BY “REAL” NOON-STATE SOURCES

Before concluding it is worth pointing out that the system generated by a “real” NOON-state source is not a pure state, as it would be in the ideal case of unitary detection efficiency. This can be shown by tracing out all the detected output modes c_{fk} and d_{fk} (with $k=1, 2, \dots, N/2$) from the density matrix obtained after applying the measurement operator of interest [either Eq. (4) or (5)] to the corresponding overall output state $|\psi_{out}\rangle$ —namely, by evaluating

$$\hat{\rho}_{a_{N/2}, b_{N/2}}^{MO \text{ real}}(\eta) = C \text{Tr}_{c_{f1}, d_{f1}, c_{f2}, d_{f2}, \dots, c_{fN/2}, d_{fN/2}} [\hat{\Pi}_{MO \text{ real}}(\eta) |\psi_{out}\rangle \langle \psi_{out}| \hat{\Pi}_{MO \text{ real}}^\dagger(\eta)], \tag{17}$$

where C is a normalization constant and “MO real” may be either Eq. (4) or (5).

Equation (17) describes the system effectively generated by “real” NOON-state sources. By evaluating the density matrix of Eq. (17) for both the single-photon detection scheme and the nondetection scheme, we find that the NOON state produced retains its coherence, but is incoherently mixed with other two-mode Fock states of the kind $|n, m\rangle\langle n, m|$, with $n, m=0, 1, 2, \dots, N-1$; in other words, the only non-null off-diagonal terms characterizing $\hat{\rho}_{a_{N/2}, b_{N/2}}^{MO \text{ real}}(\eta)$ are the ones associated with the desired NOON state. For instance, in the two-photon case, the “real” NOON-state source based on single-photon detection generates the following system:

$$\hat{\rho}_{a_1, b_1}^{2sd \text{ real}}(\eta) = C \text{Tr}_{c_{f1}, d_{f1}} [\hat{\Pi}_{2sd \text{ real}}(\eta) |\psi_{out}\rangle \langle \psi_{out}| \hat{\Pi}_{2sd \text{ real}}^\dagger(\eta)] \tag{18}$$

$$= \begin{pmatrix} \frac{(1-\eta)^2}{(2-\eta)^2} & 0 & 0 & 0 & 0 & 0 & 0 & 0 & 0 \\ 0 & \frac{1-\eta}{(2-\eta)^2} & 0 & 0 & 0 & 0 & 0 & 0 & 0 \\ 0 & 0 & \frac{1}{2(2-\eta)^2} & 0 & 0 & 0 & \frac{1}{2(2-\eta)^2} & 0 & 0 \\ 0 & 0 & 0 & \frac{1-\eta}{(2-\eta)^2} & 0 & 0 & 0 & 0 & 0 \\ 0 & 0 & 0 & 0 & 0 & 0 & 0 & 0 & 0 \\ 0 & 0 & 0 & 0 & 0 & 0 & 0 & 0 & 0 \\ 0 & 0 & \frac{1}{2(2-\eta)^2} & 0 & 0 & 0 & \frac{1}{2(2-\eta)^2} & 0 & 0 \\ 0 & 0 & 0 & 0 & 0 & 0 & 0 & 0 & 0 \\ 0 & 0 & 0 & 0 & 0 & 0 & 0 & 0 & 0 \end{pmatrix}, \tag{19}$$

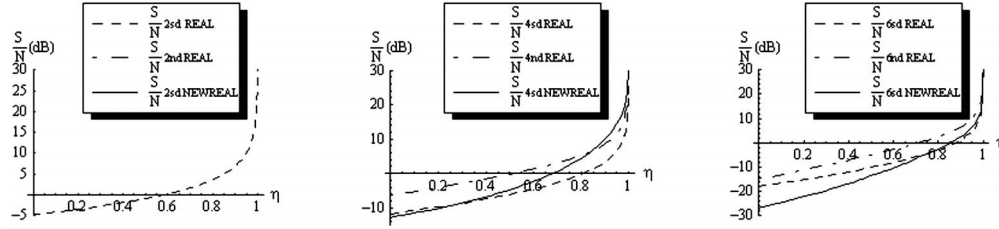


FIG. 5. Comparison of the signal-to-noise ratios (expressed in dB) characterizing “real” N -photon NOON-state sources based on N single-photon detections ($\frac{S}{N}$ Nsd real, dashed line), N nondetections (R_{Nnd} real, dash-dotted line), and $N-2$ single-photon detections (R_{Nsd} new real, solid line) for the three cases $N=2, 4, 6$ from left to right.

where the basis states are ordered in the following way: $|0, 0\rangle_{a_1, b_1}, |0, 1\rangle_{a_1, b_1}, |0, 2\rangle_{a_1, b_1}, |1, 0\rangle_{a_1, b_1}, |1, 1\rangle_{a_1, b_1}, |1, 2\rangle_{a_1, b_1}, |2, 0\rangle_{a_1, b_1}, |2, 1\rangle_{a_1, b_1}, |2, 2\rangle_{a_1, b_1}$, with $|n, m\rangle_{a_1, b_1}$ the two-mode Fock state with n photons in mode a_1 and m photons in mode b_1 ($n, m=0, 1, 2$). The density matrix in Eq. (18) is clearly an incoherent mixture of vacuum, single-photon states, and the desired NOON state with $N=2$.

Different from the above result, we find that the modified single-photon detection scheme gives rise to more coherent systems; for instance, in the $N=4$ case, the density matrix of Eq. (17) is characterized by non-null off-diagonal elements corresponding to NOON states with both $N=2$ and $N=4$.

VI. SIGNAL-TO-NOISE RATIO OF “REAL” NOON-STATE SOURCES

In view of experimental implementations of NOON-state sources, it is worth exploiting the results obtained so far for evaluating the signal-to-noise ratio characterizing a “real” NOON-state source.

We define the signal-to-noise ratio (S/N) as the ratio between the probability of producing the desired NOON state and the total probability of producing all other possible unwanted states. In order to evaluate this quantity we should sum the diagonal elements of $\hat{\rho}_{a_{N/2}, b_{N/2}}^{\text{MO real}}(\eta)$ corresponding to the desired NOON state and then divide the result by the sum of all the remaining diagonal terms. Since $\hat{\rho}_{a_{N/2}, b_{N/2}}^{\text{MO real}}(\eta)$ is normalized, we may also evaluate the single-to-noise ratio as

$$\frac{S}{N}(\eta) = \frac{\text{Tr}[\hat{\rho}_{\text{NOON}a_{N/2}, b_{N/2}}^{\text{MO real}}(\eta)]}{1 - \text{Tr}[\hat{\rho}_{\text{NOON}a_{N/2}, b_{N/2}}^{\text{MO real}}(\eta)]} = \frac{R_{\text{MO real}}(\eta)}{1 - R_{\text{MO real}}(\eta)}, \quad (20)$$

where $\hat{\rho}_{\text{NOON}a_{N/2}, b_{N/2}}^{\text{MO real}}(\eta)$ is the two-by-two “submatrix” of $\hat{\rho}_{a_{N/2}, b_{N/2}}^{\text{MO real}}(\eta)$ corresponding to the desired NOON state and its trace is just the reliability.

We carried out this analysis for each one of the three NOON-state sources considered so far; the results are reported in Fig. 5, where we chose to express the signal-to-noise ratios in dB: in this scale, positive signal-to-noise ratios indicate that the signal is larger than the noise.

Both the nondetection scheme and the modified single-photon detection scheme are characterized by the absence of noise in the case $N=2$, while the single-photon detection scheme has a positive dB signal-to-noise ratio only for detection efficiencies $\eta > 0.58$.

For $N=4$, in line with the results shown in Fig. 4, the modified single-photon detection scheme has the highest signal-to-noise ratio for values of the efficiency $\eta > 0.8$; for lower values of the efficiency, the nondetection scheme is characterized by the highest signal-to-noise ratio. In particular, the dB signal-to-noise ratio is positive for $\eta > 0.5$ in the nondetection scheme, $\eta > 0.7$ in the modified single-photon detection scheme, and $\eta > 0.8$ in the original single-photon detection scheme.

The difference between the signal-to-noise ratio associated with the nondetection scheme and the ones associated with the two single-photon detection schemes continues to be important when dealing with NOON states with $N=6$, in analogy with the result obtained for the reliability; in fact, S/N (dB) becomes positive for $\eta > 0.7$ in the nondetection scheme and for $\eta > 0.85$ in the single-photon detection scheme.

VII. CONCLUSION

By taking into account the detection losses due to the nonunitary detection efficiency of real photon counters, we have quantified both the reliability and the signal-to-noise ratio of “real” N -photon NOON-state sources for the three cases $N=2, 4, 6$. Even though further studies are required for generalizing our results to any number of photons, N , our results lead to a reevaluation of NOON-state sources based on nondetection. In fact, we have proposed and analyzed a modified version of the NOON-state source based on single-photon detection in such a way that both the nondetection and new single-photon detection schemes involve the same number of detectors ($N-2$); however, besides for the cases $N=2$ and $N=4$, the modification of the NOON-state source based on single-photon detection is not sufficient to compensate the better performances of the nondetection scheme.

Our analysis may play an important role in view of the practical implementation of both NOON-state sources and applications relying on them. However, further studies are required to quantify the effect real photon sources have on the performances of real NOON-state sources.

ACKNOWLEDGMENTS

The authors thank V. Berardi, J. P. Dowling, J. Franson, T. Pittman, M. H. Rubin, Y. H. Shih, and G. Scarcelli for useful suggestions and stimulating discussions. This research was supported in part by Università degli Studi di Bari e INFN-Sezione di Bari.

- [1] J. J. Bollinger, W. M. Itano, D. J. Wineland, and D. J. Heinzen, *Phys. Rev. A* **54**, R4649 (1996).
- [2] C. C. Gerry and R. A. Campos, *Phys. Rev. A* **64**, 063814 (2001).
- [3] H. Lee, P. Kok, N. J. Cerf, and J. P. Dowling, *Phys. Rev. A* **65**, 030101(R) (2002).
- [4] X. Zou, K. Pahlke, and W. Mathis, e-print arXiv:quant-ph/0110149.
- [5] J. Fiurásek, *Phys. Rev. A* **65**, 053818 (2002).
- [6] P. Kok, H. Lee, and J. P. Dowling, *Phys. Rev. A* **65**, 052104 (2002).
- [7] G. J. Pryde and A. G. White, *Phys. Rev. A* **68**, 052315 (2003).
- [8] F. Shafiei, P. Srinivasan, and Z. Y. Ou, *Phys. Rev. A* **70**, 043803 (2004).
- [9] P. Walther, J.-W. Pan, M. Aspelmeyer, R. Ursin, S. Gasparoni, and A. Zeilinger, *Nature (London)* **429**, 158 (2004).
- [10] M. W. Mitchell, J. S. Lundeen, and A. M. Steinberg, *Nature (London)* **429**, 161 (2004).
- [11] H. Wang and T. Kobayashi, *Phys. Rev. A* **71**, 021802(R) (2005).
- [12] F. W. Sun, B. H. Liu, Y. F. Huang, Z. Y. Ou, and G. C. Guo, *Phys. Rev. A* **74**, 033812 (2006).
- [13] B. Liu and Z. Y. Ou, *Phys. Rev. A* **74**, 035802 (2006).
- [14] A. E. B. Nielsen and K. Molmer, *Phys. Rev. A* **75**, 063803 (2007).
- [15] K. T. Kapale and J. P. Dowling, *Phys. Rev. Lett.* **99**, 053602 (2007).
- [16] C. H. Bennett and B. D. DiVincenzo, *Nature (London)* **404**, 247 (2000); N. Gisin and R. Thew, *Nat. Photonics* **1**, 165 (2007).
- [17] A. N. Boto, P. Kok, D. S. Abrams, S. L. Braunstein, C. P. Williams, and J. P. Dowling, *Phys. Rev. Lett.* **85**, 2733 (2000); M. D'Angelo, M. V. Chekhova, and Y. Shih, *ibid.* **87**, 013602 (2001).
- [18] Z. Y. Ou, *Phys. Rev. A* **55**, 2598 (1997).
- [19] C. K. Hong, Z. Y. Ou, and L. Mandel, *Phys. Rev. Lett.* **59**, 2044 (1987); Y. H. Shih and C. O. Alley, *ibid.* **61**, 2921 (1988).
- [20] L. De Caro and A. Garuccio, *Phys. Rev. A* **54**, 174 (1996).
- [21] A. Peres, *Phys. Rev. A* **61**, 022116 (2000).
- [22] P. G. Kwiat, A. M. Steinberg, R. Y. Chiao, P. H. Eberhard, and M. D. Petroff, *Phys. Rev. A* **48**, R867 (1993).
- [23] G. Di Giuseppe, M. Atatüre, M. D. Shaw, A. V. Sergienko, B. E. A. Saleh, M. C. Teich, A. J. Miller, S. W. Nam, and J. Martinis, *Phys. Rev. A* **68**, 063817 (2003).